REMOTE VERSUS IN SITU TURBULENCE MEASUREMENTS

Walter Frost
FWG Associates, Inc.
Tullahoma, Tennessee

Comparisons of in situ wind and turbulence measurements made with the NASA B-57 instrumented aircraft and those remotely made with both radar and lidar systems are presented. Turbulence measurements with a lidar or radar system as compared with those from an aircraft are the principal themes. However, some discussion of mean wind speed and direction measurements is presented.

First, the principle of measuring turbulence with Doppler lidar and radar is briefly and conceptually described. The comparisons with aircraft measurements are then discussed. Two studies in particular are addressed: One uses the JAWS Doppler radar data and the other uses data gathered both with the NASA Marshall Space Flight Center (NASA/MSFC) and the NOAA Wave Propagation Laboratory (NOAA/WPL) ground-based lidars. Finally, some conclusions and recommendations are made.

Figure 1 illustrates conceptually how Doppler radars and lidars measure winds. A pulse of microwave energy is transmitted into the atmosphere. The beam of energy spreads out in a conical manner. The transmitted signal is scattered back to a receiver by raindrops or, in clear air, by aerosols, bugs, or other materials which scatter back the signal. The signal is then recorded and processed. The volume element in space which the radar probes is conical in shape. It gets bigger as it moves out. The length of the volume element for a pulsed radar or lidar system is equal to the speed of sound, c, times the pulse duration, τ, divided by 2. Each volume element is called a range gate. There are several range gates that extend outward in space until the transmitted signal is too weak for further radiation to be scattered to the receiver. Typically τ is 1 μs, and with the speed of light being 300,000 m/s the range gate length is 150 m long. The length varies based on the system capabilities, and for lidars it is often 300 m long. Therefore, it is quite a long volume in space that the system interrogates. The lateral spread of the beam, d, depends on the divergence angle, θ, and the distance from the transmitter. The diameter of the volume element is thus variable becoming larger further from the transmitter. For radar the spread rate may be on the order of 17 m/km.

The signal scattered back to the receiver is from those particles which are within the volume element. The particles are assumed to move in equilibrium with the air and thus at the mean wind speed. Of course, due to turbulence and wind shear across the volume element, the particles will also be relative to one another.

The radar system signal processor records the Doppler frequency shift due to the velocity component of the particles away from or toward the receiver. The Doppler frequency is then related to each individual particle motion by the relationship $f_d = -2v_{ri}/\lambda$ where v_{ri} is the velocity component of

the ith particle along the direction of the beam (i.e., the radial velocity component). The mean wind is essentially the average of the sum of all these motions. The subscript r in Figure 1 denotes the radial component either toward or away from the radar.

The processed signal of the Doppler frequency shift due to each particle is idealized as having a Gaussian shape. Thus, the signal represents a frequency spectrum. If the majority of the particles are moving with the mean air motion, then the most energy is scattered at the value of the mean Doppler shift frequency, f_d (see Figure 1). The mean frequency shift is then correlated with the mean velocity. Due to the fact that the particles are also moving randomly relative to one another because of the turbulence and other air motions, there is a spreading of the energy associated with the f_d. Thus, different amounts of energy are associated with different frequencies depending on how the particles are moving relative to each other. If you assume the signal is Gaussianly distributed, then a standard deviation (called the pulse standard deviation), σ_p (see Figure 1), can be defined and, in principle, is a measure of the chaotic motion due to turbulence within the volume element being sampled. Thus, the standard deviation of the Gaussian distribution or the spectral width of the return signal should be a measure of the atmospheric turbulence.

A pulsed lidar works on the same principle. A typical Doppler frequency shift spectrum from a lidar is shown in Figure 2. In practice, the signal does not have the nice Gaussian distribution that is assumed and generally several pulse signals are averaged to get meaningful results. If the pulse repetition is 100 cycles/sec and ten pulse returns are averaged, a 10 millisecond average measure of the wind is obtained.

Thus, with a radar or lidar measurement you are averaging the wind both spatially and with time which could be 0.5 to 2 seconds depending on how many pulses are averaged to obtain a good strong return. The beam spreading of a lidar is much smaller than that of a radar. The lidar signal at most spreads about 1 m for the range achievable. In effect, the spatial volume sensed by a lidar can be considered as a pencil line approximately 100 to 300 m long.

The spreading or spectral width of the time average signal for the lidar is also a measure of turbulence, i.e., the pulse standard deviation, σ_p. In turn, a time history of 0.5 to 2 seconds averaged wind speeds can be plotted from the lidar data as illustrated in Figure 2. From this time history, a standard deviation of the wind, σ_w, can be computed by conventional techniques. Thus, two standard deviations will be discussed; one is σ_p which represents the second moment or spectral width of the Doppler frequency lidar signal distribution and the other one is σ_w which is calculated as illustrated by the equation in Figure 2. Both measurements remember are turbulence averages over a relatively large spatial region in space due to the volume resolution of the radar or lidar.

Figure 3 is a sketch (approximately to scale) of a typical volume element that is 5 km from the transmitter at which point the volume element is 150 m long and 85 m in diameter. The size of a B-57 type aircraft relative to volume element is illustrated. The radar volume element overwhelmingly

engulfs the entire aircraft. In turn, the lidar beam is more like a line through space, 300 m long.

To compare the aircraft measurement of turbulence, which is effectively a point measurement, with Doppler radar or lidar, you must fly along the beam and compare the data measured in each range gate with that measured by the aircraft while it is in or next to that portion of the beam (see Figure 4). The aircraft measurement is essentially the turbulence measured point by point along a line of flight. The different sampling volumes cause some problems in interpreting what turbulence is actually being compared. The aircraft turbulence intensity will, in general, be small because we compare measurements only for the period of time when the aircraft is "beside" the individual range gates. The time for an aircraft to travel the length of a range gate is about 1.5 to 2 seconds. Thus, when we compute the mean for each 1.5 to 2 second turbulence record, the mean is really turbulence itself. Turbulence intensities defined in this manner will be small compared to values computed typically from 45-minute to one-hour records normally reported in the literature.

In considering the pulse volume standard deviation, there are physical factors other than turbulence, which will cause the second moment of the Doppler signal frequency spectrum to broaden. Figure 4 lists four factors which cause spectral broadening. Various correction factors are also shown in the figure.

If there is a gradient in mean wind (i.e., wind shear) across the volume element, spectral broadening will occur. The magnitude of spectral broadening due to wind shear is estimated by the expression for σ_s in Figure 5.

There will be spectral broadening due to the fact that the radar is generally scanning. As the radar beam moves through space, spectral broadening occurs. Finally, there is spectral broadening from raindrops having different fall rates. The value of σ_t is of interest to our study. Therefore, it is necessary to correct the overall pulse spectral width, σ_p, by subtracting σ_s, σ_α, and σ_d. The radar data have been corrected in this paper, but the lidar data have not. At the bottom of Figure 5 you can again see the definition of the wind standard deviation as contrasted to the pulse standard deviation at the top of the figure.

First, some of the comparisons of aircraft data with Doppler-radar-measured turbulence are presented. Second-moment data from JAWS are used. Three cases are considered. During the JAWS Project in Colorado, three Doppler radars were used to measure the wind field throughout a huge volume in space. The location of these volumes is shown in Figure 6. The volumes are typically 2 km high and their areal extent is as illustrated in the figure. For the July 14 case, the region indicated on the figure was probed with both the CP-2 and CP-4 radars located as shown. Velocities from two directions for an overlapping volume in space were available from this experiment. During the JAWS Project, the NASA B-57 aircraft was flown in the experiment region to gather data on gust gradient across the wing span, which is described in Murrow's paper [1]. Although we were principally gathering data relatively to gust gradients, the opportunity to use the data for comparisons with Doppler

radar turbulence measurements is a fringe benefit. Unfortunately, the only time flights actually coincided with the particular dual Doppler measurement was for the July 14 case. The problem we encountered in trying to operate the aircraft during the JAWS Project was that the JAWS experimental region encompassed Stapleton International Airport, Denver, Colorado. If there was any interesting weather like microbursts or thunderstorm activity, the aircraft was vectored out of that region because of traffic control problems. We, therefore, never really got the opportunity to fly repeatedly where the Doppler radar was probing a region that contained the aircraft flight path.

The July 14 case is the best data set available. For this case, three runs, Runs 23, 24, and 25, from Flight 6, as shown on Figure 7, were available where the aircraft flew through or close to the region the radar was scanning at that moment. Run 23 occurred slightly before the Doppler measurement was made. Run 24 corresponds exactly with the time the measurement was made. Run 25 also corresponds in time with the Doppler radar measurement but it is somewhat outside the radar volume element.

Characteristics of the flight path for Run 24, Flight 6, are shown in Figure 8. The flight occurred at approximately 6500 ft altitude which is about 500 to 600 ft above the terrain. The terrain was relatively uniform. The aircraft was flying in the direction indicated in the upper right-hand corner of the figure. A strong tailwind was encountered during this particular phase of the flight as shown by the arrows which represent one-second average horizontal wind vectors along the flight path during the run.

Figure 9 shows the results of the comparison of the turbulence measurements. The crosses are the second-moment data from the radar at each volume element or range gate. Strictly speaking, it is not exactly the value in each volume element. The data we used was provided to us by NCAR. The σ_p values were interpolated to a 200 m square grid system from the initial radial wind speed data. The zero's on the figure are the wind standard deviation, σ_w, which we calculated from the radar data from the formula given in Figure 7. The symbols *, L, and V are longitudinal, lateral, and vertical (relative to the aircraft) turbulence standard deviations. The aircraft measurements, in general, correspond with the wind standard deviation values. Notice that the values are low compared with normally reported values. This is because each σ represents the standard deviation about a spatial mean for the 150 m section of wind corresponding to the range gate or volume element through which the airplane flies.

The pulse volume standard deviation, σ_p, is higher than the other values by at least a factor of 2. The reason for this is not fully understood at this time. If the standard deviation for the three velocity components are computed from the total time history (87 seconds) while the airplane flies the entire length of the flight path for the July 14 case (i.e., not just through each range gate) and if the square root of the turbulence kinetic energy is taken as an effective value of σ, good agreement with the radar pulse standard deviation is achieved. I am not sure as of yet how to interpret this. Jean Lee from NOAA/NSSL compares dissipation rates, which are a measure of turbulence kinetic energy with their Doppler radar second-moment measurements.

Figure 10 offers an explanation of possibly why there is a major difference between radar turbulence and aircraft-measured turbulence. When you measure turbulence with an aircraft, even if you go right through the radar volume element, you are basically making point measurements along a line, say path A in the figure. There is some mean wind speed along that line in space during the period required to fly the path. The aircraft turbulence intensity reported here is the fluctuations about that particular mean. If we flew through another part of the volume element, say along path B, you might see quite a different mean wind speed or distribution about that mean for the short period of time required to fly along the path. The second-moment data from the radar, on the other hand, is an effective total spatial average throughout the entire volume element. The radar measurement is representative of the turbulence within that volume element because it is a spatial measurement. If we had a long enough time record and Taylor's hypothesis is valid, the aircraft measurement should, in principle, give the same result. The time records we are working with, however, are very short and work needs to be done to learn how to handle non-stationary turbulence resulting from sampling over very short times or regions of space.

Next, the Doppler lidar turbulence meaurements are addressed. Three studies have been carried out. The February 7 and 9 study is described here. This study was funded by NASA Goddard and carried out at Boulder, Colorado. Two things were of interest: (1) Measuring turbulence flux parameters relative to mountain-induced flows and (2) making comparisons with the NOAA/WPL ground-based lidar. Again, the NASA B-57 aircraft was used; the program was a joint effort between NASA Goddard (who provided the funds), NASA Langley (who reduced the data), NASA Dryden (who operated the aircraft), and NASA Marshall (who directed the program).

The flight patterns flown during the lidar comparison test are shown on Figure 11. The NOAA/WPL lidar was set up on Table Mountain. Interest was in turbulence due to winds blowing over the mountains and parallel to the mountains, respectively. The lidar beam was directed at approximately 4.5° elevation and 200° azimuth and an approach was made along this trajectory. The aircraft would then make a turn and at the same time the lidar beam was rotated to a 290° azimuth at the same 4.5° elevation. The aircraft would then climb out along that line of sight. Our intent was to make enough flights along each trajectory to do ensemble averaging. Turbulence in the boundary layer is not homogeneous, particularly over or in the vicinity of mountains. Several samples of turbulence corresponding to each range gate (roughly 300 m) was needed in order to analyze the data by ensemble averaging techniques. Roughly ten samples for each 300 m increment in space is needed. Ensemble statistical analysis can then be carried out with the data. That was the plan. However, Doppler lidar data of the time resolution needed was not recorded at corresponding times with flights as frequently as planned. Thus, we had a limited data set.

Figure 12 is a cross section in space of the lidar beam path relative to the terrain for the 4.5° elevation and 290° azimuth orientation. Each vertical line represents a range gate (300 m long). Data were taken at 0.5 seconds, i.e., pulsing 12 times per second and averaging six pulse returns. The vectors plotted along vertical lines are the time histories of 0.5-second

averaged wind speeds. The vector length represents the magnitude of the wind speed and time is plotted in the vertical direction. In this particular case, the wind was getting stronger with time. The arrowheads show that there is a reverse flow over this mountain which is interesting. The wind is blowing toward the left-hand side of the figure in the upper range gates and is blowing to the right-hand side in the lower range gates. The flow pattern corresponds to a wake region such as readily observed in laboratory studies. Mountain flows obviously have flow separation regions as can be seen in these data.

Tables 1 and 2 list the data sets analyzed. The plan was to obtain eight to ten runs along each lidar beam so we could do ensemble averaging. However, we only got six for February 7 and four for February 9. In principle, to do ensemble statistics these are not enough records. However, if that is all the data you have, then you try to do the best you can.

Figures 13 and 14 show results from the February 7 and February 9 data sets. Mean wind speed (average wind speed for the period of time the aircraft is in that 300 m volume element) is compared with the time history from the radar signal for that same period of time in the left-hand side figures. There's general agreement here which we think is very good. You cannot expect one to one agreement since it is impossible to fly the aircraft directly along the beam. Moreover, because of the presence of the mountains, which can block or shed the wind, not measuring the wind at exactly the same region in space can cause large differences. Note also that because of the short averaging times of 1.5 to 3 seconds, the reported wind speed, are in themselves low-frequency turbulence.

The difference between Doppler mean winds and aircraft mean winds was on the order of 2 m/s. There are several other factors besides terrain effects and large-scale turbulence that could contribute to these differences. The inertial navigation system has a Schuler drift. If you are on the high side of the Schuler oscillation you can easily be 2 m/s off in inertial velocity. Also, one of the problems we were having with the lidar during this test was the pulse transmission frequency was varying slightly which would give a velocity error relative to the reference frequency. The right-hand side of that figure shows the measured turbulence intensity. A "*" designates aircraft-measured turbulence defined as previously described and a "+" designates the lidar spectral width turbulence. We did not take the wind shear out of the lidar data, and you will notice this right away. There is a very pronounced peak in the pulse volume data at corresponding positions of wind shear.

As with the radar data, the second moment data are roughly a factor of 2 greater than the aircraft data and the wind standard deviation data. I did not expect the lidar results to be a factor of 2 or 3 higher than the aircraft data because the beam from the lidar is at most 1 m thick in conical shape. Thus, the spatial volume sampled is small compared to the Doppler radar, which can have a sampling volume greater than 85 m in thickness. An explanation as to why the second-moment or spectral broadening of the lidar data are so much larger than the aircraft measurements is not presently clear.

Figure 15 shows turbulence spectra computed from the data. There is quite a bit of scatter in these data because of ensemble averaging of only a limited number of runs. The "*" represents the turbulence spectrum calculated using the aircraft data. The open circles are the spectra computed from the lidar data. In general, these agree pretty much with one another over the region where they overlap. The lidar is actually 0.5-second averages. With 0.5-second data, the maximum frequency that can be resolved is 1 Hz. The lidar data then have a frequency range from 1 Hz to about 0.01 Hz whereas the aircraft data, where we were sampling 40 times per second, range from 20 Hz to about 0.04 Hz. Typically, the computed spectrum follow roughly a -5/3 slope.

Preliminary conclusions are that lidar- and radar-measured winds generally agree with the aircraft-measured winds. Differences in agreement could be due to problems with comparing spatial and temporal data, Schuler drift in the INS system or to variation in the pulse transmission frequencies from the lidar system.

Not only does the magnitude of the winds agree reasonably well but also the profile shapes, in general, correspond. Other results from the NASA/MSFC lidar that are even better than these are available because at Marshall we made eight to ten runs with which we could carry out ensemble averaging. The results look quite a bit better. It is also concluded that the wind standard deviation turbulence intensity and aircraft standard deviations are in good agreement. This conclusion is based on the fact that the intensity is the correct order of magnitude and the spectrum overlap a -5/3 slope and follow. Maybe good agreement is too strong, but they are in agreement.

The spectral width or second-moment data which come directly from the radar or lidar signal is about two or three times larger than the aircraft measurement for both the lidar and radar. The reasons may be due to the fact that the radar is looking at a very large volume and the turbulence is a spatial measurement whereas the airplane is sampling along a line in space. Study is required, however, to resolve this difference. The variation of the spatial width standard deviation with height is very similar to the wind standard deviation and aircraft standard deviation values.

Recommendations are to plan and carry out research to fully resolve the issue of turbulence measurements with lidar and radar to establish a physical understanding of the temporal and spatial resolution of the turbulence data measured. There needs to be work done, although I understand there is work being done by the USAF/Geophysics Lab and NOAA/NSSL, in developing algorithms for operationally predicting or forecasting turbulence. Finally, I see great hope for the use of Doppler radar and lidar in numerical forecasting. If the point is ever reached where turbulence flux models are incorporated into these computational techniques and they are updated periodically with measurements, as currently done for wind speed and direction, it would be very useful to develop a scanning method using the Doppler lidar or radar which would provide measured momentum flux and perhaps heat and mass flux, also. The flux models in the numerical codes could then be updated routinely with actual measurements.

Reference

1. Murrow, Harold N.: Measurements of Atmospheric Turbulence, NASA CP-2468, pp. 73-92, 1987.

COMMENT: C. M. Tchen (City College of New York). It is found in atmospheric turbulence that the energy spectrum does not necessarily follow the Kolmogoroff -5/3 law, but it is often modified into the -1 law by wind shear. I noticed that your data in strong wind shear also show a milder slope than the -5/3 slope. The -1 spectrum can be broadened by the presence of rain or snow because of the added air-particle interaction. The recent turbulence measurements in the atmospheric surface layer in Scandinavian and the Russian laser measurements in atmospheric precipitation show this deviation from the Kolmogoroff law.

FROST: How were those measurements made?

TCHEN: The ORESUND Experiments 1985 by the northern European countries measured the atmospheric turbulence by means of a variety of instrumentations: hot-wire anemometers, cup anemometers, Doppler sodars, radiosonde microwave radiometers, and balloons. The Russian experiments measured the atmospheric turbulence in precipitation by means of laser intensity fluctuations.

QUESTION: Dave Emmitt (Simpson Weather Associates). Due to the length-to-diameter ratio of the lidar beam, at Marshall we tried to look at the difference in interpretation when we looked downwind versus crosswind with our beam and found there was some difference. You were looking at 200° and 290°. Did you detect any difference in trying to interpret data for those two directions?

FROST: We didn't look specifically at that problem but, if the effect was present, it was not obvious.

QUESTION: Bob McClatchey (AFGL). You didn't say much about clouds and precipitation in your comments. Lidar can't see through clouds and precipitation; radar has the hope of doing that. It wasn't obvious either whether the radars that were used in the Colorado experiment were looking at hydrometeors or whether they were looking at clear air and index of refraction changes. Can you comment on that, and whether in that context you conceive of a dual system involving both radar and lidar to really look at the whole regime? What's the maximum altitude range you can get with such ground-based systems.

FROST: There was no rain or clouds in any of our experiments. The radar returns for the data we looked at were clear-air returns. As you say, the radar does look through the clouds and the lidar will not. If there is any cloud cover, then your measurements are basically limited to the elevation of the cloud cover with the lidar system.

TABLE 1. Selected Runs of the February 7 Test.

B-57B Aircraft Data			NOAA Lidar Data		
Run No.	Azimuth Angle	Sampling Time (MST) Start to End	PRF (Hz)	Number of Pulse Average	Sampling Time (MST) Start to End
2	290	11:46:42-11:49:19	12	6	11:46:53-11:49:04
3	200	11:56:42-12:00:27	12	6	11:57:59-12:00:06
4	290	12:02:03-12:03:59	12	6	12:00:50-12:02:55
5	200	12:12:01-12:15:56	12	6	12:12:17-12:16:41
6	290	12:17:48-12:21:29	12	6	12:16:43-12:19:50
7	200	12:27:51-12:31:49	12	6	12:27-00-12:29:35

TABLE 2. Selected Runs of the February 9 Test.

B-57B Aircraft Data			NOAA Lidar Data		
Run No.	Azimuth Angle	Sampling Time (MST) Start to End	PRF (Hz)	Number of Pulse Average	Sampling Time (MST) Start to End
9	200	12:14:06-12:17:45	12	48	12:13:39-12:17:23
10	290	12:19:30-12:23:09	12	24	12:17:45-12:22:13
11	200	12:28:05-12:31:43	12	24	12:28:49-12:30:53
12	290	12:33:25-12:37:09	12	24	12:33:47-12:36:49

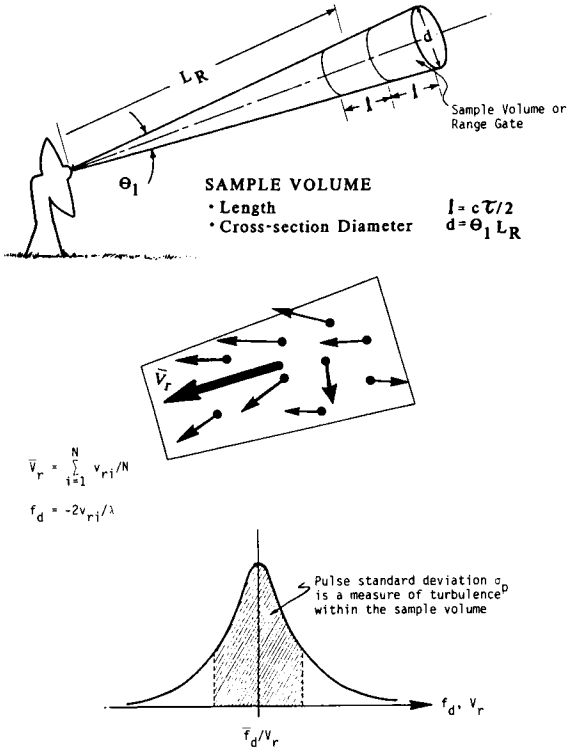

Figure 1. Doppler radar.

LIDAR SIGNAL SPECTRUM

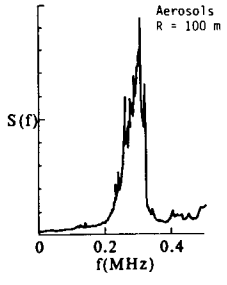

SEVERAL SPECTRA ARE AVERAGED TO GIVE THE MEAN WIND SPEED AND SPECTRAL WIDTH. TYPICAL AVERAGING TIMES ARE 0.5 to 2 SECONDS.

TIME HISTORY OF RADIAL VELOCITY

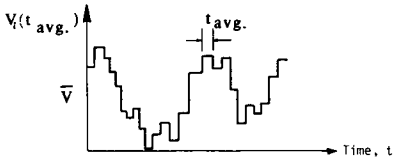

WIND STANDARD DEVIATION

$$\sigma_w = \sum_{i=1}^{N} (V_i(t_{avg}) - \bar{V})/N$$

Figure 2. Lidar signal.

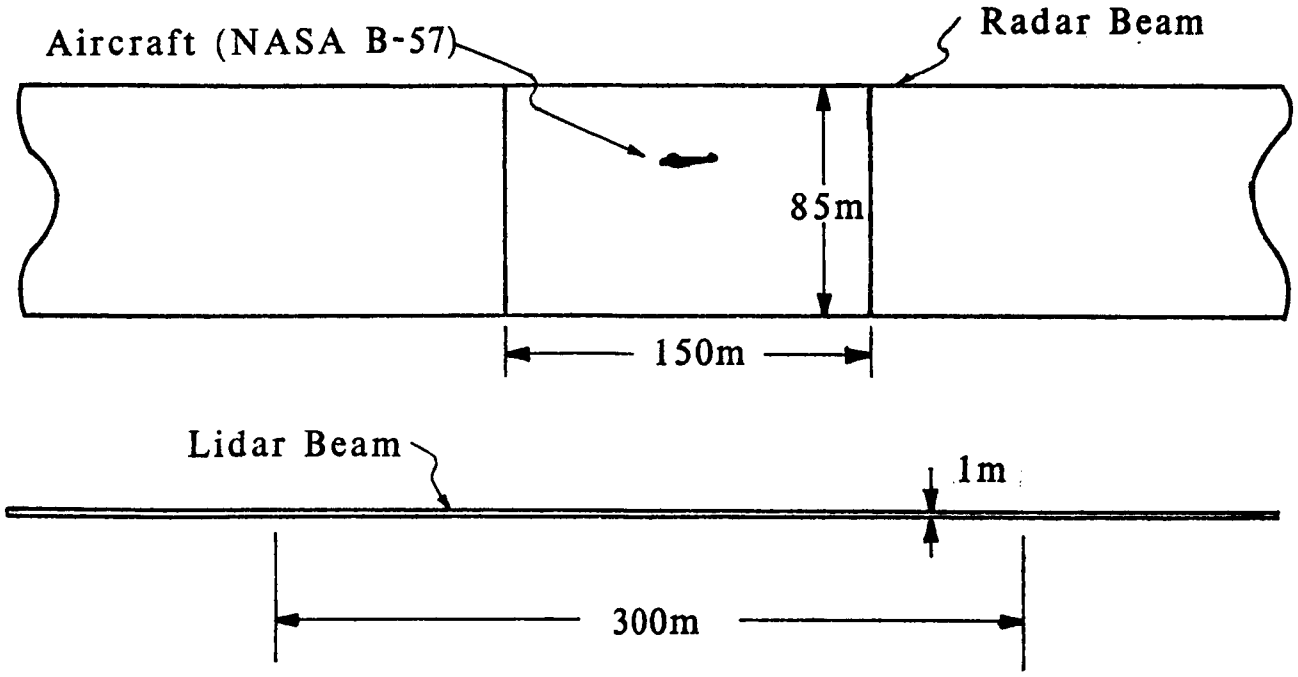

Figure 3. Sketch of relative sizes of aircraft, radar beam, and lidar beam. Scale 1 in = 50 m.

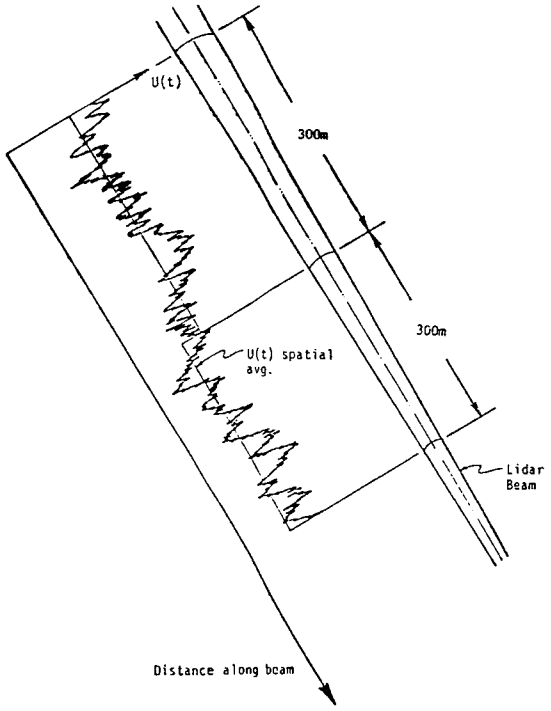

Figure 4. Aircraft measures turbulence along a line in space as compared to a lidar or radar which measures a spatial averaged turbulence in a conical volume element.

PULSE SD

- $\sigma_p = (\sigma_s^2 + \sigma_t^2 + \sigma_\alpha^2 + \sigma_d^2)^{1/2}$ in a pulse volume

where

σ_s = broadening due to radial wind shear

$= [(\sigma_r K_r)^2 + (R_o \sigma_\theta K_\theta)^2 + (R_o \sigma_\phi K_\phi)^2]^{1/2}$

σ_t = turbulence intensity

σ_α = broadening due to antenna motion

$= (\alpha\lambda \cos \theta_e / 2\pi\theta_1)\sqrt{\ell n 2}$

σ_d = contribution of different speeds of fall for various sized drops

$= \sigma_{do} \sin \theta_e$

$\sigma_\theta^2 = \sigma_\phi^2 = \theta_1/(16\ell n 2)$

$\sigma_r^2 = (0.35\ c\tau/2)^2$

WIND SD

- $\sigma_w = \left(\frac{1}{N} \Sigma(V_r^2 - \overline{V_r^2})\right)^{1/2}$ in a grid volume (200 m x 200 m x 200 m)

Figure 5. Turbulence intensity.

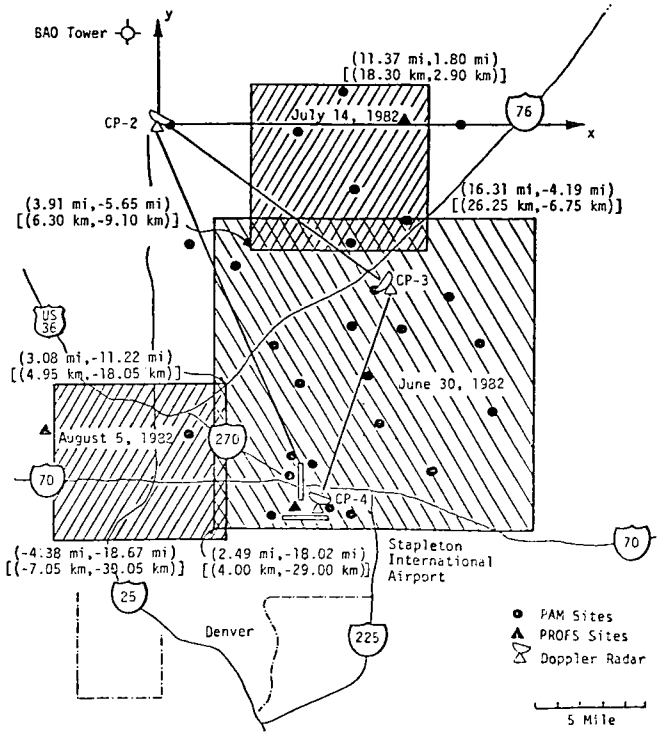

Figure 6. Location of spatial region for which JAWS data are available.

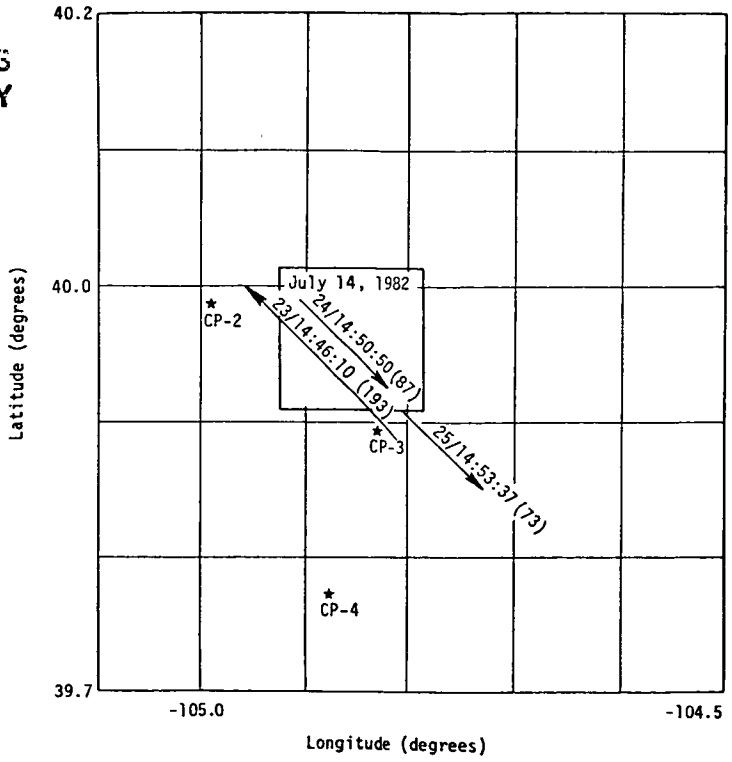

Figure 7. Relative positions of the JAWS July 14, 1982, microburst and the flight paths of Runs 23, 24, and 25 in Flight 6 of NASA B-57B aircraft.

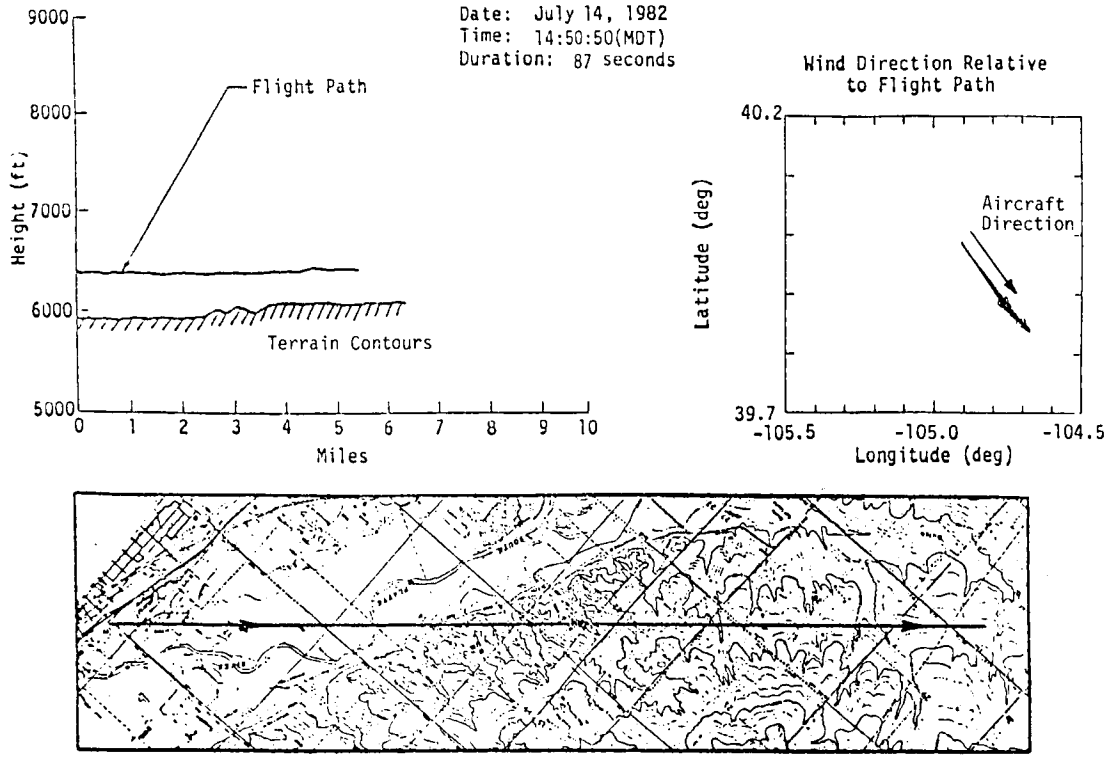

Figure 8. Flight path information: Flight 6, Run 24.

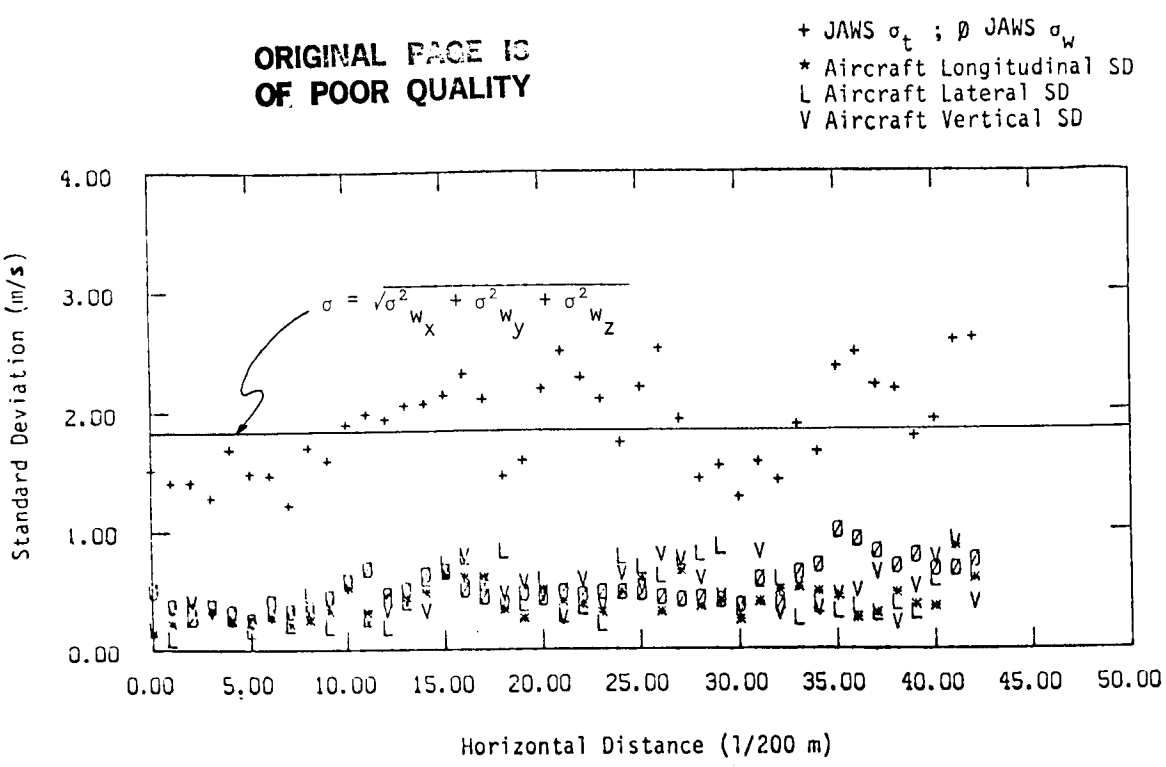

Figure 9. Comparison of σ_t with calculated turbulence intensities from NASA B-57B measurement (Run 24).

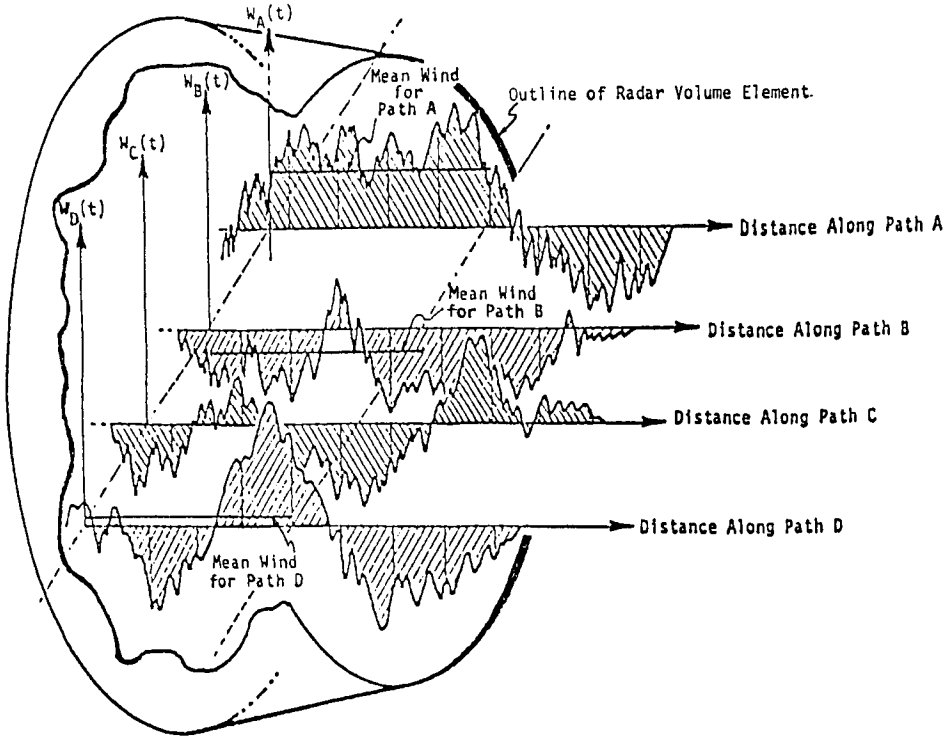

Figure 10. Schematic illustration of spatial extent of turbulence measurements from an aircraft and from a radar.

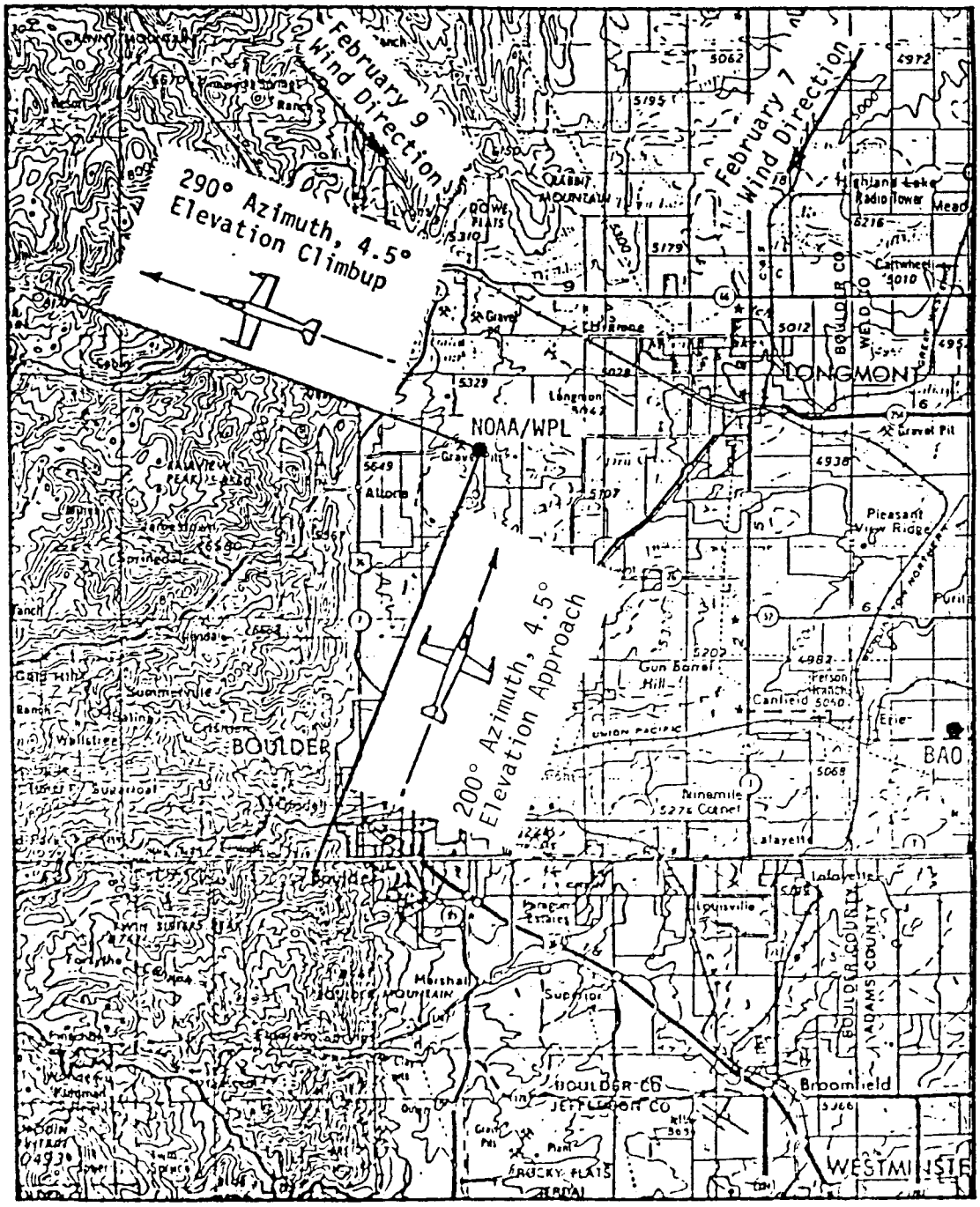

Figure 11. Flight paths relative to the lidar beam at 200° and 290° azimuth, respectively, at Boulder, Colorado, February 7 and 9, 1984.

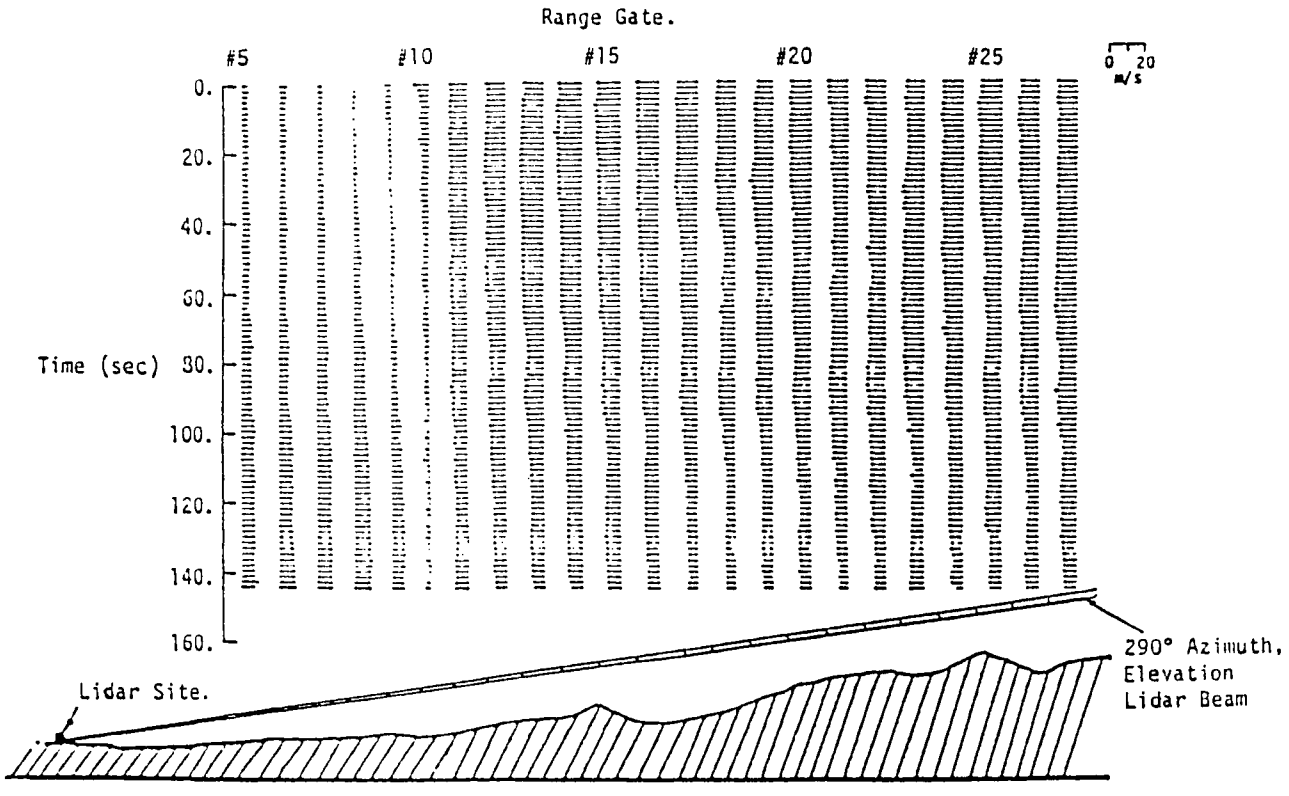

Figure 12. Time history of lidar-measured wind vector at 290° azimuth, 4.5° elevation relative to the terrain on February 9, 1984, Boulder, Colorado.

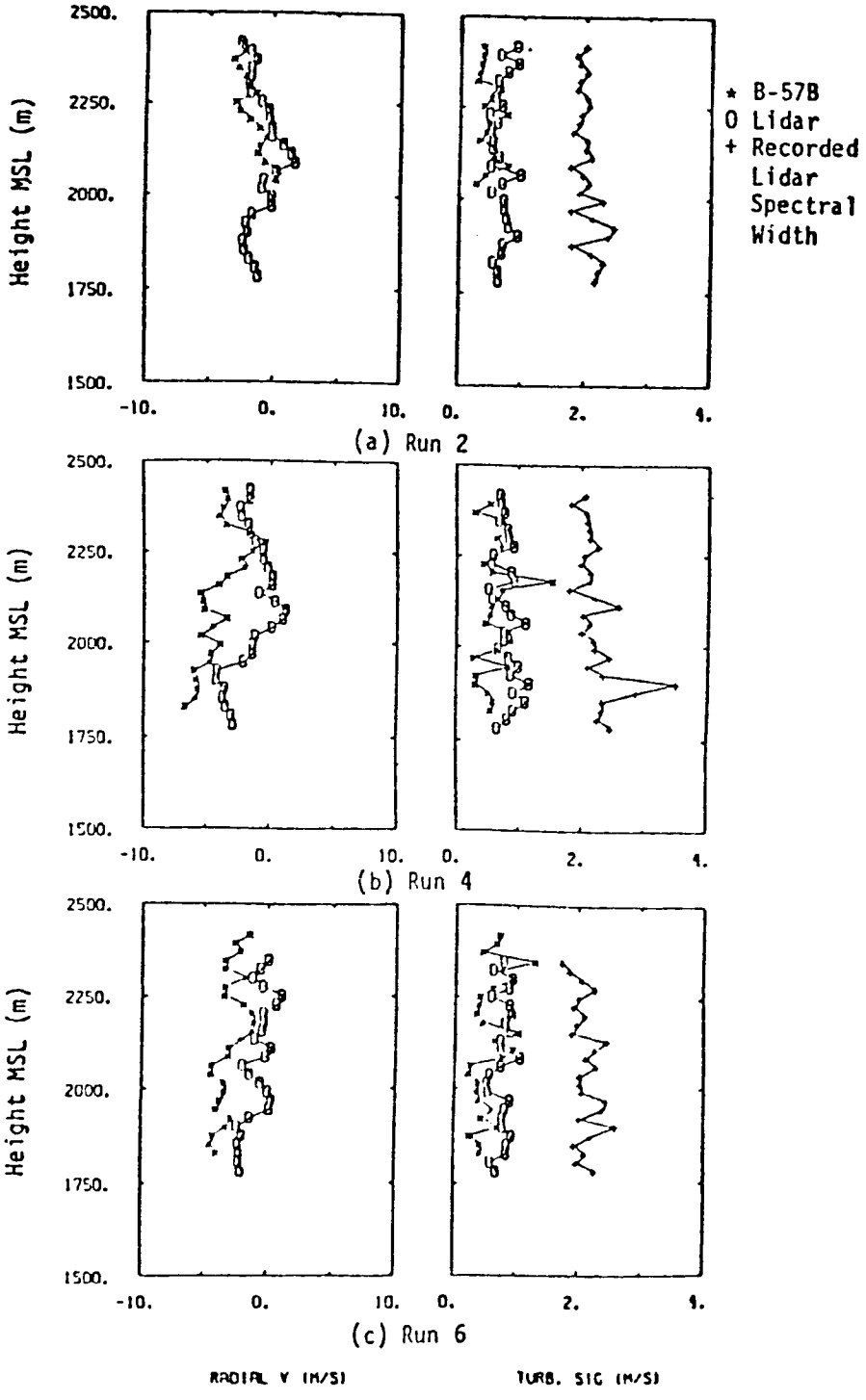

Figure 13. Comparison of radial mean wind velocity, calculated turbulence intensity, and lidar spectral width between aircraft measurement and lidar measurement on February 7, 1984 (280° azimuth).

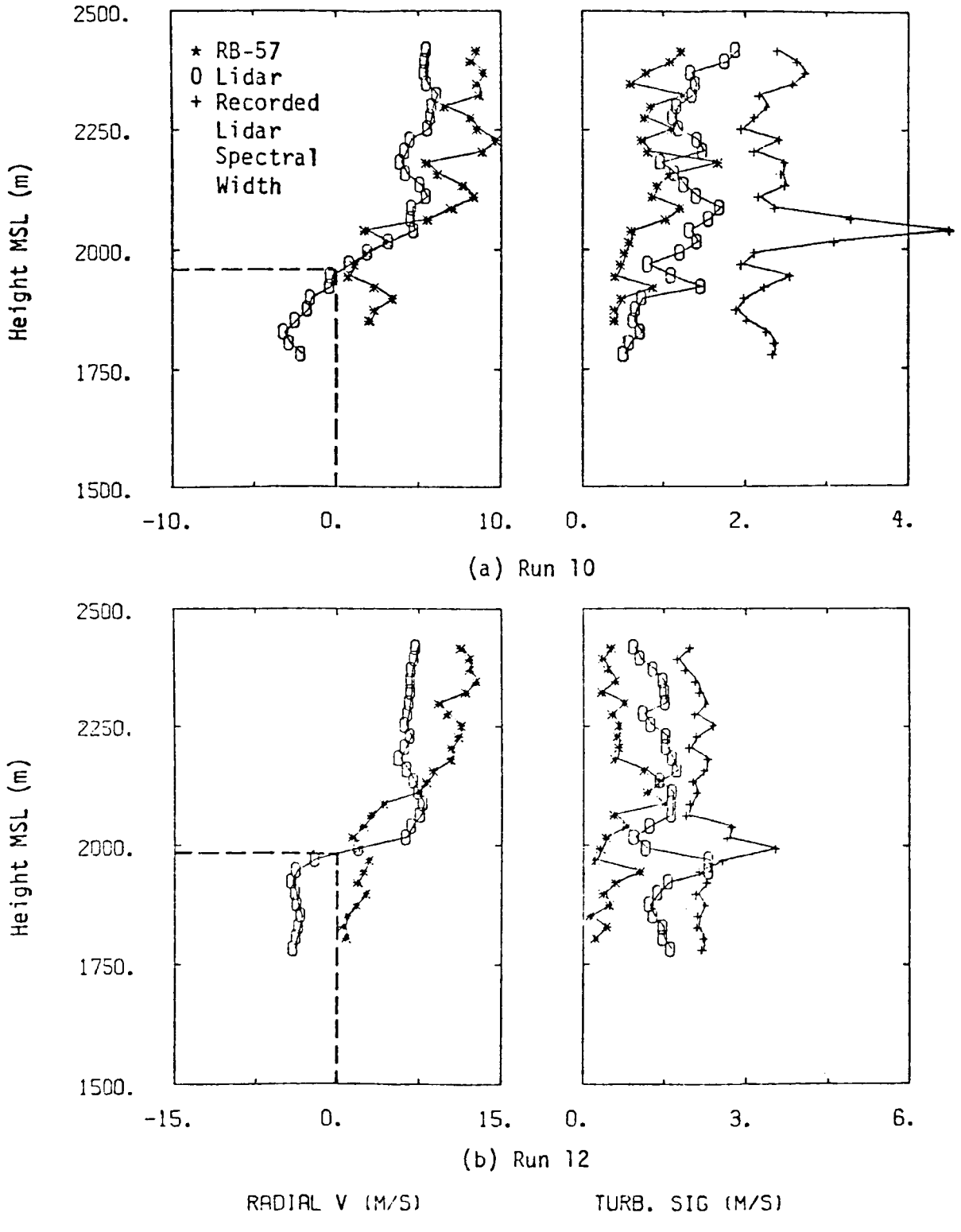

Figure 14. Comparison of radial mean wind velocity, calculated turbulence intensity, and lidar spectral width between aircraft measurement and lidar measurement on February 9, 1984 (290° azimuth).

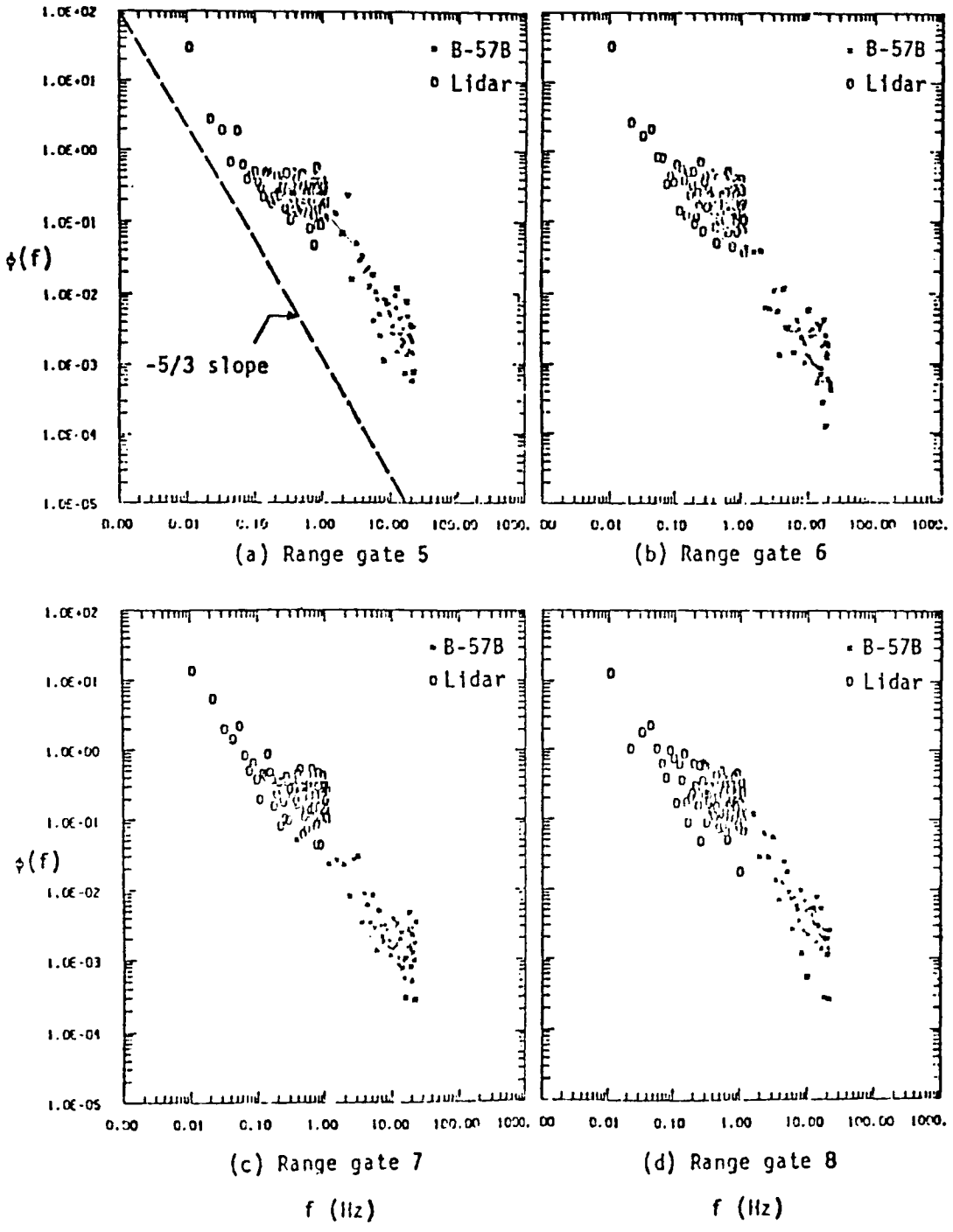

Figure 15. Computed radial turbulence spectra at 200° azimuth path.